Journal of Marine Science and Technology

Volume 17 | Issue 4 Article 7

# AEROSOL OPTICAL DEPTH RETRIEVAL FOR SPOT HRV IMAGES

Chien-Hui Liu
*Department of Information Management/Geographic Information Management and Research Center, Transworld Institute of Technology, Douliu, Yunlin 64045, Taiwan, R.O.C.*, chliu@mail.tit.edu.tw

Gin-Rong Liu
*Center for Space and Remote Sensing Research, National Central University, Jhongli City, Taoyuan County 32001, Taiwan, R.O.C.*



Recommended Citation
Liu, Chien-Hui and Liu, Gin-Rong (2009) "AEROSOL OPTICAL DEPTH RETRIEVAL FOR SPOT HRV IMAGES," *Journal of Marine Science and Technology*: Vol. 17: Iss. 4, Article 7.
DOI: 10.51400/2709-6998.1986
Available at: https://jmstt.ntou.edu.tw/journal/vol17/iss4/7

# AEROSOL OPTICAL DEPTH RETRIEVAL FOR SPOT HRV IMAGES

## Acknowledgements

This work was partially supported by the National Science Council of Taiwan under grant NSC 95-2221-E-265 -001. The second author would like to thank Dr. Lin T. H. in CSRSR, NCU for his help in maintaining NCU_Taiwan site of AERONET. The authors are grateful to NASA/GSFC for contribution to this research.

# AEROSOL OPTICAL DEPTH RETRIEVAL FOR SPOT HRV IMAGES

Chien-Hui Liu* and Gin-Rong Liu**

Key words: aerosol optical depth, sunphotometer, SPOT.


## ABSTRACT

Atmospheric aerosol is an important factor of the Earth's radiation budget. The aerosol optical depth (AOD) is also the key parameter in generating surface products from remotely sensed data. An image-based retrieval algorithm of aerosol characteristics and surface reflectance is used to retrieve the AOD from SPOT satellite images in this paper. The accuracy of retrieved AOD is assessed using sunphotometer measurements. SPOT satellite images in Jhongli , Taoyuan county are used to testify the algorithm. The results show that the root-mean-square error (RMSE) of the retrieved AOD at 0.55 $\mu$m is 0.10. Over the range of measured AOD 0.08~0.34, the mean relative error is 49%. The RMSE of the retrieval is very sensitive to assumed DT reflectance: it can be reduced to 0.067, when assumed DT reflectance in green band is set 0.035, instead of 0.03. Urban aerosol model is not suitable in this test area, because of its high absorption. The RMSE of retrieved AOD is insensitive to continental, maritime and biomass-burning aerosol models, since the deviation of RMSE of the retrieved AOD using these three models is within 0.02. The errors are also shown to be independent of the measured AODs. More observations over different locations and canopy species are required to testify the algorithm in the future.


## I. INTRODUCTION

Aerosol plays an important role in the radiative forcing of the earth's climate through a direct effect of scattering and absorption of atmospheric radiation, and an indirect effect acting as cloud condensation nuclei [16, 17, 25]. An increase in the tropospheric aerosol optical depth (AOD) of 0.1 would decrease the temperature about 1°C on Earth surface [9]. Risk of hospital admissions may be increased by air pollution and duststorms [5] due to long-range transport [19, 20]. Since the remotely sensed signal is modulated by the atmosphere, AOD is also necessary for atmospheric correction of remotely sensed data. An error of 0.01 in assumed surface reflectance can cause error of 0.1 in retrieved AOD [15]. It is also reported that an increase in AOD of 0.2 can decrease the surface reflectance of 0.02 in green band of SPOT high resolution visible (HRV) for target reflectance of 0.03, when AOD is 0.33 [22]. For quantitative remote sensing, most inversion algorithms are based on surface reflectance [11, 18].

Owing to its highly spatial-temporal variability, remote sensing of aerosol characteristics is a fundamentally difficult problem [6]. Currently, retrieval of aerosol mainly relies on the use of dark targets (DT) [13, 14, 26]. The error of retrieved AOD due to the errors of the assumed reflectances over DT can be expected to be much lower than those over bright targets, owing to larger atmospheric reflectance in top-of-atmosphere (TOA) signal for DTs. The major limitation to the application of this method is the presence of pixels fully covered by DTs [13]. If in lack of mid-IR bands, such as SPOT HRV and FORMOSAT-2 Remote Sensing Instrument (RSI), DTs can be identified as the pixels with low near-IR signal and high vegetation index [13, 22]. By taking advantage of the low opacity of most aerosol types in the mid-IR bands of Moderate Resolution Imaging Spectroradiometer (MODIS) aboard both NASA's Terra and Aqua satellites, DTs can be identified globally. The reflectances of DTs in the blue and red bands can be estimated using high correlation with the reflectance in mid-IR band (2.13 $\mu$m) [14]. Extended DT method has also been developed to be applicable for brighter targets [26]. It keeps the same accuracy as the original version of the DT method. Alternatively, the contrast reduction method derives AOD without using DTs. Based on the assumption of stable surface reflectance with time, variations in TOA reflectance can be attributed to the changes of atmospheric optical properties [21, 28, 30]. The application of optimal distance number into the structure function method has been greatly improved the accuracy of the retrieved AOD from NOAA Advanced Very High Resolution Radiometer (AVHRR) data [24]. This method will be limited for its application worldwide, owing to the assumption of unchanged surface reflectance within neighborhoods and high contrast between them [18].

In this paper, an image-based retrieval algorithm of aerosol characteristics and surface reflectance [22, 23] is used to re-

*Paper submitted 01/23/08; revised 09/03/08; accepted 10/21/08. Author for correspondence: Chien-Hui Liu (e-mail: chliu@mail.tit.edu.tw).*

**Department of Information Management/Geographic Information Management and Research Center, Transworld Institute of Technology, Douliu, Yunlin 64045, Taiwan, R.O.C.*

***Center for Space and Remote Sensing Research, National Central University, Jhongli City, Taoyuan County 32001, Taiwan, R.O.C.*

trieve AOD from SPOT satellite images. This method had been applied to atmospheric correction of SPOT HRV images [22]. The RMSE of the retrieved surface reflectance is 0.02. It had been also successfully applied to the retrieveal of AOD over Landsat TM images [23]. The mean errors of the retrieved AODs are 0.14 and 0.05 in TM1 and TM3 bands. Unfortunately, the accuracy of the retrieved AODs by SPOT HRV images is never assessed. In this study, SPOT satellite images in Jhongli city, Taoyuan county and concurrent sunphotometer measurements are used to testify this method. Sensitivity of the retrieval to assumed reflectance of DT and aerosol model is also studied.

## II. METHODOLOGY

### 1. Modeling of TOA Reflectance

Let us consider that the surface is uniform and Lambertian. If gas absorption is neglected, TOA reflectance $\rho^{\mathrm{TOA}}$ received by a satellite sensor for a target reflectance $\rho$ at sea level altitude under solar and viewing zenith angles $\theta_s$, $\theta_v$ and relative azimuthal angle $\phi$ can be written as [29]:

$$\rho^{\mathrm{TOA}}(\mu_s,\mu_v,\phi) = \rho_a(\mu_s,\mu_v,\phi) + T(\mu_s)T(\mu_v)\frac{\rho}{1-\rho S}, \quad (1)$$

where $\mu_s$ and $\mu_v$ are $\cos\theta_s$ and $\cos\theta_v$, $\rho_a$ is the atmospheric reflectance, $T(\mu_s)$ and $T(\mu_v)$ are the downward and upward total scattering transmittances given by $T(\mu) = e^{-\tau/\mu} + t_d(\mu)$, $t_d(\mu)$ is the diffuse transmittance, $\tau$ is the atmospheric optical depth including molecular scattering and aerosol, and $S$ is the spherical albedo of the atmosphere. Functions of $t_d(\mu)$ and $S$ can be well approximated by Eddington method [31] as following:

$$t_d(\mu) = \exp(-\tau/\mu)\left\{\exp\left[(0.52\tau_r + \beta_d\tau_a)/\mu\right] - 1\right\}, \quad (2)$$

$$S = (0.92\tau_r + \alpha_r\tau_a)\exp(-\tau), \quad (3)$$

$$\alpha_r = 1 - g, \quad (4)$$

$$\beta_d = (1+g)/2, \quad (5)$$

where $g = \langle\cos\Theta\rangle$ is the asymmetry factor, $\Theta$ is the scattering angle and defined as:

$$\cos\Theta = -\mu_s\mu_v - \left(1-\mu_s\right)^{1/2}\left(1-\mu_v\right)^{1/2}\cos\phi. \quad (6)$$

$\rho_a$ is determined by the modified subroutine ATMREF in 5S [29]. The functions $\rho_a$, $t_d$ and $S$ are all functions of AOD $\tau_a$ and aerosol optical properties, including single scattering albedo $\omega_0$, phase function $P_a(\Theta)$ and $g$ which can be determined by Mie theory [12]. In practice, Wiscombe's code [32] is used. Its inputs include aerosol size distribution and complex refractive index (CRI). Junge size distribution is adopted here and its exponent is set to be the average value, i.e. 3.0 [7, 12]. The size range is considered to be 0.01~10 $\mu$m. The value of aerosol CRI is set to be 1.5322-0.01174i corresponding to continental type in [22, 23].

### 2. AOD Retrieval Algorithm

To retrieve the AOD from remotely sensed data by equation (1), an image-based algorithm is applied [22, 23]. It is based on DT algorithm as suggested by Kaufman and Sendra [13]. DTs can be identified as the pixels with low near-IR signal and high vegetation index. The digital counts for AOD retrieval are determined from the very sharp increase in the lower bound of the histogram of DTs in the green and red bands [4, 22]. Their corresponding surface reflectances $\rho$ are set to be 0.03 and 0.02 in green and red bands of SPOT images [13]. Based on the assumed aerosol size distribution and CRI, $\omega_0$, $P_a(\Theta)$ and $g$ can be then determined by Mie theory as mentioned above. These aerosol optical parameters are used to determined $\rho_a$, $t_d$ and $S$, using modified ATMREF in 5S as well as (2) and (3). Lookup table of satellite-measured $\rho^{\mathrm{TOA}}$ as a function of $\tau_a$ for a DT is then used to derive AOD in green and red band of HRV. Because of the highly spatial-temporal variability of aerosol, the algorithm is modified for non-uniform aerosol effect [23] by dividing the image into blocks following the work of Richter [27]. For every block, uniform aerosol effect is assumed and the above procedures are performed to retrieve AOD.

### 3. Test Site and Sunphotometer Measurements

The sunphotometer, located on the roof of Center for Space and Remote Sensing Research (CSRSR), National Central University (NCU) [21], serves as NCU_Taiwan station, one of the Aerosol Robotic Network (AERONET) global observation sites [10], providing a long-term, continuous and public domain database of aerosol optical depth and radiative properties. The longitude, latitude and elevation of this site are 24.96667° North, 121.19167° East and 171.0 meter. The station is situated at western rural area of Jhongli city in northern Taiwan. It is surrounded by many land-cover types, including mainly vegetation such as rice paddy field, water ponds and some build-up lands (Fig. 1). Hence, it is very appropriate to be selected to testify the algorithm based on DT.

The sunphotometer of AERONET can provide spectral AOD at several wavelengths including 0.34, 0.38, 0.44, 0.67, 0.87 and 1.02 $\mu$m. The basic principle of AOD retrieval by a sunphotometer is by observation of direct sun extinction. The AOD can be derived from the Beer's law written as [3]:

$$I(\lambda) = I_0(\lambda)\exp[-\tau^*(\lambda)m(\theta_s)], \quad (7)$$

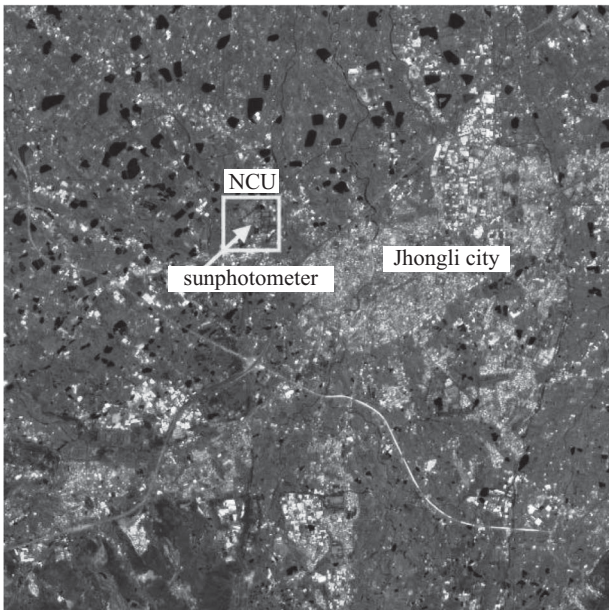


**Fig. 1. SPOT HRV image of test area obtained on 27 June 1998.**

where $I_0(\lambda)$ is the extraterrestrial flux corrected by earth-sun distance at wavelength $\lambda$, $I(\lambda)$ is the measured flux reaching the ground and $m$ is the air mass factor $1/\mu_s$; the total atmospheric optical depth $\tau^*$ can be written as:

$$\tau^*(\lambda) = \tau_r(\lambda) + \tau_a(\lambda) + \tau_g(\lambda), \tag{8}$$

where $\tau_g(\lambda)$ is the optical depth due to absorption by gases such as ozone, nitrogen dioxide, carbon dioxide, methane and water vapor. To obtain $\tau_a(\lambda)$ from measured $\tau^*(\lambda)$, $\tau_r(\lambda)$ and $\tau_g(\lambda)$ need to be estimated. Detailed information of estimation of $\tau_r(\lambda)$, $\tau_g(\lambda)$ and $m$ as well as other ancillary data set, including gas contents and atmospheric pressure, to retrieve AOD can be found in [1] and references therein. To prevent from possible cloud contaminated data, quality-assured level 2.0 AOD data, i.e. clear-sky data, are used in this study and downloaded from website http://aeronet.gsfc.nasa.gov/new_web/index.html.

## 4. SPOT Satellite Images and Measured AOD Dataset

A dataset of five SPOT images, collected in CSRSR NCU, are used to testify the algorithm (Table 1). They range from 27 June 1998 to 20 September 2000. The solar zenith angles are 20.6°~42.5°, and the viewing zenith angles are 3.6°~30.3°. The viewing direction is in back-scattering region if the relative azimuth is smaller than 90°. There are three images scanned from back-scattering region. Since all of the images are in clear sky, the algorithm is applied under the assumption of uniform aerosol effect. In spite of a limited database, it is also helpful to assess the algorithm.

The values of concurrently measured AODs are from 0.10 to 0.46 at 0.44 $\mu$m (Table 2). Among these five dates, the clearest sky is on 13 October 1999, and the haziest sky is on 20 September 2000. In order to validate the algorithm, the measured AOD at 0.55 $\mu$m is interpolated from measured AODs at 0.44 and 0.67 $\mu$m by Ångstrom formula [2]:

$$\tau_a(\lambda) = b\lambda^{-\alpha}, \tag{9}$$

where $b$ is the Ångstrom turbidity coefficient and $\alpha$ is the wavelength exponent. In practice, by taking the logarithm of both side in equation (9), $\alpha$ can be written as:

$$\alpha = -\frac{\ln[\tau_a(\lambda_{0.44})/\tau_a(\lambda_{0.67})]}{\ln(\lambda_{0.44}/\lambda_{0.67})}. \tag{10}$$

Then AOD at 0.55 $\mu$m can be obtained by:

$$\tau_a(\lambda_{0.55}) = \tau_a(\lambda^*)(\lambda_{0.55}/\lambda^*)^{-\alpha}, \tag{11}$$

where $\lambda^*$ can be either $\lambda_{0.44}$ or $\lambda_{0.67}$. Likewise, the retrieved AOD at 0.55 $\mu$m can be interpolated from those in green and red bands of SPOT HRV by (9)-(11).

**Table 1. The geometric parameters of SPOT HRV image set used in this study. All angles are in degrees.**

| Date | Solar zenith angle | Viewing zenith angle | Relative azimuth angle |
|---|---|---|---|
| 27 Jun. 1998 | 20.6 | 30.3 | 13.8 |
| 8 Nov. 1998 | 42.5 | 13.1 | 119.8 |
| 13 Oct. 1999 | 36.2 | 25.5 | 46.5 |
| 21 Oct. 1999 | 37.0 | 3.6 | 124.7 |
| 20 Sep. 2000 | 29.0 | 17.2 | 52.8 |

**Table 2. The measured aerosol optical depths from sunphotometer at various wavelengths for the SPOT image set in Table 1.**

| Date | 0.44 $\mu$m | 0.67 $\mu$m | 0.87 $\mu$m | 1.02 $\mu$m |
|---|---|---|---|---|
| 27 Jun. 1998 | 0.38 | 0.19 | 0.12 | 0.11 |
| 8 Nov. 1998 | 0.42 | 0.25 | 0.17 | 0.14 |
| 13 Oct. 1999 | 0.10 | 0.06 | 0.05 | 0.05 |
| 21 Oct. 1999 | 0.29 | 0.18 | 0.13 | 0.12 |
| 20 Sep. 2000 | 0.46 | 0.25 | 0.16 | 0.15 |

## III. RESULTS AND DISCUSSION

Comparison of sunphotometer measurements and retrieved AODs from SPOT HRV both at 0.55 $\mu$m is shown in Table 3. The maximum error is 0.14, which is in the haziest sky on 20 Sep. 2000. The minimum error is -0.02, whose AOD is 0.22 on

**Table 3. The AODs at 0.55 μm of both sunphotometer measurements and the retrieval from SPOT HRV images in Table 1. Ångstrom formula is used to obtain AOD at 0.55 μm. The root mean square error is 0.10. The mean relative error is 49%.**

| Date | Sunphoto-meter | SPOT | Error | Relative error (%) |
|---|---|---|---|---|
| 27 Jun. 1998 | 0.26 | 0.35 | 0.09 | 34 |
| 8 Nov. 1998 | 0.32 | 0.41 | 0.09 | 29 |
| 13 Oct. 1999 | 0.08 | 0.20 | 0.12 | 151 |
| 21 Oct. 1999 | 0.22 | 0.20 | -0.02 | -11 |
| 20 Sep. 2000 | 0.34 | 0.45 | 0.14 | 42 |

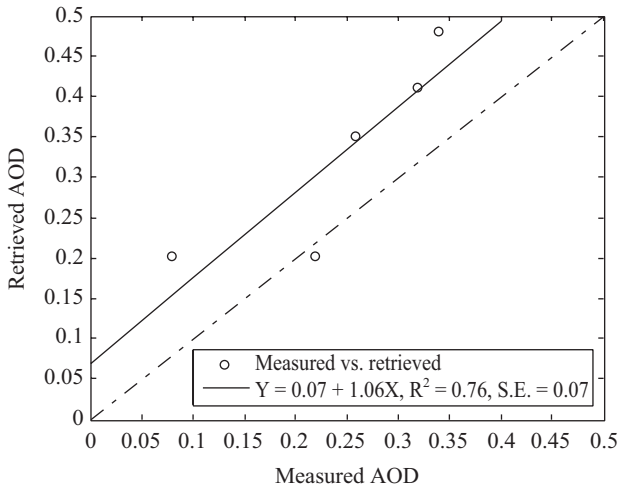


**Fig. 2. Comparison of sunphotometer measurements and retrieval of AOD at 0.55 μm. Data are depicted in Table 3. S.E. is the standard error of estimate of the least squares fitted line.**

21 Oct. 1999. To better know the relationship, the measurements and retrieved values are also plotted (Fig. 2). Linear least squares result is also shown. The slope is 1.06 and the intercept is 0.07. The value of $R^2$ is 0.76. The discrepancy of the measurement and the retrieval may be due to the assumed DT reflectances in green band $\rho_{DTG}$ and red band $\rho_{DTR}$ as well as the assumed aerosol microphysical properties such as CRI and Junge exponent. Although the mean relative error is 49%, the RMSE of the retrieval is 0.10 (Table 3). Although the relative error of retrieved AOD on 13 Oct. 1999 can be up to 151%, which is much larger than the average relative error of 49%, the absolute error is 0.12, which is about the RMSE of the retrieval in the current dataset. As shown later, the error may be attributed to the error due to assumption of DT reflectances and certainly to the low aerosol loading with AOD of 0.08 only.

To better understand the sensitivity of the accuracy to assumed DT reflectances and aerosol properties, the errors as a function of $\rho_{DTG}$ for different aerosol models are studied (Fig. 3). The errors are considered for the current entire dataset. In addition to continental aerosol, maritime, urban and biomass-burning aerosol models are also considered. The value of $\rho_{DTG}$ is assumed to range from 0.02 to 0.05 and the value of $\rho_{DTR}$ is assumed to be 0.02 only. This is because $\rho_{DTR}$ is lower and more stable than $\rho_{DTG}$. The RMSE of retrieved AOD is much higher, i.e. larger than 0.7, for all assumed DT reflectances $\rho_{DTG}$ when urban aerosol model is assumed; however, it can be as low as 0.07, 0.07 and 0.06 respectively, when continental, martime and biomass-burning aerosol models are assumed and $\rho_{DTG}$ is assumed to be 0.035. It seems that three considered aerosol models are all suitable for this dataset at this test site, except urban aerosol model, since the deviation of RMSEs for these three aerosol models is only within 0.02 for all assumed $\rho_{DTG}$. The failure of urban aerosol is due to its high absorption, i.e. $\omega_0$ of 0.65; however, the values of $\omega_0$ for the other three aerosol models are similar and larger than 0.95 [29]. Retrieved AOD is also over-estimated, when urban aerosol model is considered at this test site, which is consistent with the study in [22]. On the other hand, the RMSEs of retrieved AOD are very sensitive to the assumed $\rho_{DTG}$. They decrease from 0.200 to 0.067 as $\rho_{DTG}$ increases from 0.02 to 0.035, and then increase to 0.213 as $\rho_{DTG}$ increases to 0.05 if continental aerosol model is assumed. Similar behavior and amount of RMSEs are also shown as biomass-burning or maritime aerosol model is assumed. Sensitivity of AOD retrieval error to $\rho_{DTG}$ is about -10, which is similar to the results shown in [15] and [22] as afore-mentioned. Hence, the RMSE of AOD retrieval for the current dataset can be reduced from 0.10 to 0.067 as $\rho_{DTG}$ increase from 0.03 to 0.035, when continental aerosol model is assumed; it can be 0.072 or 0.063 respectively, when maritime or biomass-burning aerosol model is assumed.

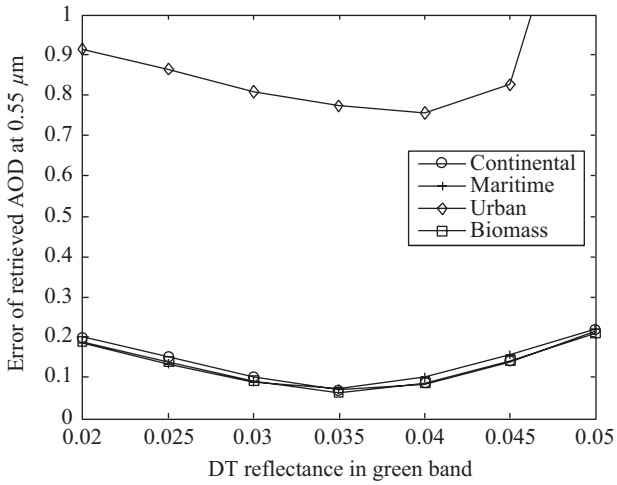


**Fig. 3. The root-mean-square errors of retrieved AOD at 0.55 μm for the dataset as a function of assumed DT reflectance in green (XS1) band for different aerosol models.**

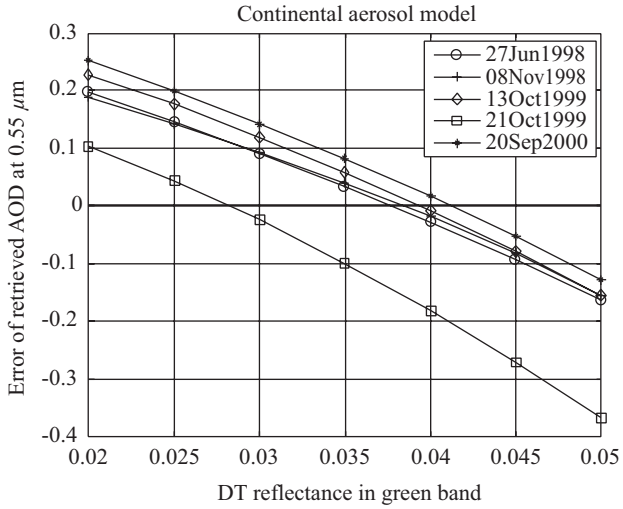


**Fig. 4. The error of retrieved AOD at 0.55 μm for every image as a function of assumed DT reflectance in green (XS1) band for continental aerosol model.**

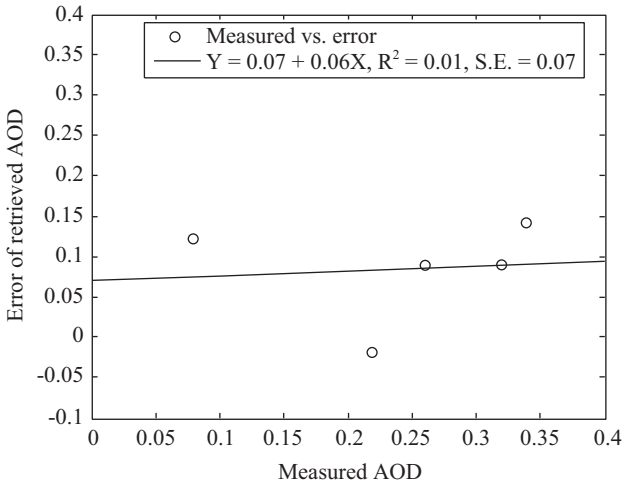


**Fig. 5. Plot of dependence of retrieved AOD error on measured AOD. Data are depicted in Table 3. S.E. is the standard error of estimate of the least squares fitted line.**

It would be also interesting to study the error of AOD retrieval for different $\rho_{DTG}$ in every image (Fig. 4). As mentioned above, the deviation of RMSEs of AOD retrieval for the current dataset is only within 0.02 for maritime, continental and biomass-burning aerosol models, only continental aerosol model is considered. The error can be minimized, when $\rho_{DTG}$ are within the range from 0.037 to 0.042 on the four dates except 21 Oct. 1999. $\rho_{DTG}$ on 21 Oct. 1999 is about 0.028 and is closest to the original assumed $\rho_{DTG}$ of 0.03. This may be due to both growth stage of vegetation and bidirectional effect. It has been shown that reflectances in green and red edge regions are sensitive to chlorophyll content of vegetation [8]. Reflectance in green band is lowest, when chlorophyll content reach a maximum for soybean and maize. Growth parameters of rice plants, e.g. leaf area index, reach the maximum near heading when the vegetative growth was greatest, and decreased thereafter [33]. Heading occurs approximately at 70 days after transplanting in the 2nd crop season over Wufeng village, Taichung in central Taiwan. Since the rice crop is transplanted around in the beginning of August over test area, it seems reasonable that $\rho_{DTG}$ reaches a minimum on 21 Oct. 1999 compared with those on four other dates. The other reason for lowest $\rho_{DTG}$ on 21 Oct. 1999 may be due to bidirectional effect. The viewing zenith angle is about nadir ($3.6^0$) on that date, while it is greater than $13^0$ on the other dates. Because of the larger portion of cast shadow viewed by the sensor at nadir direction, $\rho_{DTG}$ is lowest among the entire dataset. However, an extensive dataset containing data from different locations and canopy species are required to test the accuracy of the algorithm. Based on the current result, it is suggested that a feasible assumption of $\rho_{DTG}$ ranging from 0.03 to 0.04 can be used. Average value of $\rho_{DTG}$ 0.035 can be assumed if there is no ancillary information about the vegetation growth stage or bidirectional effect of the canopy.

Finally, it is also interesting to note that the error is 0.12 on 13 Oct. 1999, i.e. the clearest day, which is comparable to that on 20 Sep. 2000, i.e. the haziest day. To clarify if the algorithm can be applicable for different haziness, the relationship between the errors of the retrieved AODs and measurements is shown in Fig. 5. The slope of the linear fitted line is 0.06 and the value of $R^2$ is 0.01, which indicates the errors of the retrieved values are independent on the measured AODs. Hence, the algorithm can be suitable for different haziness.

## IV. CONCLUSION

The accuracy of an algorithm to retrieve AOD for SPOT images is presented in this paper. Five SPOT images collected in CSRSR NCU are implemented. Concurrent sunphotometer measurements over the same area are used to testify the algorithm. The results show that the RMSE of the retrieved AOD at 0.55 μm is 0.10. The mean relative error is 49% over the range of AOD 0.08~0.34. Except for urban aerosol model, which is high absorptive, the RMSE of retrieved AOD is insensitive to continental, maritime and biomass-burning aerosol models. Sensitivity study has shown that the retrieval error is very sensitive to assumed DT reflectance in green band. RMSE can be reduced from 0.10 to 0.067, when assumed $\rho_{DTG}$ is set from 0.03 to 0.035. It is suggested that if more ancillary information is available about the vegetation growth stage or bidirectional effect of the canopy for DT, assumed $\rho_{DTG}$ can be selected from 0.03 to 0.04. Otherwise, average value (0.035) in $\rho_{DTG}$ can be assumed. $\rho_{DTR}$ is assumed to be 0.02, which it is lower and more stable than $\rho_{DTG}$. The errors are also shown to be independent of the measured AODs. Hence, the algorithm appears quite satisfactory for different haziness in this dataset. In the future, more observations are required to fully testify the algorithm over different areas and canopies, especially over urban for its potential application on air pollution monitoring [21].

## ACKNOWLEDGMENTS

This work was partially supported by the National Science Council of Taiwan under grant NSC 95-2221-E-265 -001. The second author would like to thank Dr. Lin T. H. in CSRSR, NCU for his help in maintaining NCU_Taiwan site of AERONET. The authors are grateful to NASA/GSFC for contribution to this research.

## REFERENCES

1. "AERONET Direct Sun Algorithm – Version 2" downloaded from http://aeronet.gsfc.nasa.gov/new_web/Documents/version2_table.pdf.
2. Ångstrom, A., "The parameters of atmospheric turbidity," *Tellus*, Vol. 16, pp. 64-75 (1964).
3. Bodhaine, B. A., Wood, N. B., Dutton, E. G., and Slusser, J. R., "On rayleigh optical depth calculations," *Journal of Atmospheric and Oceanic Technology*, Vol. 16, pp. 1854-1861 (1999).
4. Chavez, P. S., "An improved dark-object subtraction technique for atmospheric scattering correction of multispectral data," *Remote Sensing of Environment*, Vol. 24, pp. 459-479 (1988).
5. Chen, Y., Sheen, P., Chen, E., Liu, Y., Wu, T., and Yang, C., "Effects of Asian dust storm events on daily mortality in Taipei, Taiwan," *Environmental Research*, Vol. 95, pp. 151-155 (2004).
6. Dubovik, O., Holben, B., Eck, T. F., Smirnov, A., Kaufman, Y. J., King, M. D., Tanré, D., and Slutsker, I., "Variability of absorption and optical properties of key aerosol types observed in worldwide locations," *Journal of the Atmospheric Sciences*, Vol. 59, pp. 590-608 (2002).
7. Fraser, R. S. and Kaufman, Y. J., "The relative importance of aerosol scattering and absorption in remote sensing," *IEEE Transactions on Geoscience and Remote Sensing*, Vol. 23, pp. 625-633 (1985).
8. Gitelson, A. A., Viña, A., Ciganda, V., Rundquist, D. C., and Arkebauer, T. J., "Remote estimation of canopy chlorophyll content in crops," *Geophysical Research Letter*, Vol. 32, L08403, doi:10.1029/2005GL022688 (2005).
9. Hansen, J. E. and Lacis, A. A., "Sun and dust versus greenhouse gases: an assessment of their relative roles in global climate change," *Nature*, Vol. 346, pp. 713-719 (1990).
10. Holben, B. N., Eck, T. F., Slutsker, I., Tanre, D., Buis, J. P., Setzer, A., Vermote, E., Reagan, J. A., Kaufman, Y., Nakajima, T., Lavenu, F., Jankowiak, I., and Smirnov, A., "AERONET - a federated instrument network and data archive for aerosol characterization," *Remote Sensing of Environment*, Vol. 66, pp. 1-16 (1998).
11. Huang, S. J., Liu, G. R., and Kuo, T. H., "The atmospheric correction of ROCSAT-1 OCI imagery - Part I: OCITRAN-1," *Terrestrial, Atmospheric and Oceanic Sciences*, Vol. 10, pp. 855-864 (1999).
12. Kaufman, Y. J., *Theory* and *Applications of Optical Remote Sensing*, John Wiley & Sons, New York, pp. 336-428 (1989).
13. Kaufman, Y. J. and Sendra, C., "Algorithm for atmospheric corrections," *International Journal of Remote Sensing*, Vol. 9, pp. 1357-1381 (1988).
14. Kaufman, Y. J., Tanre, D., Remer, L. A., Vermote, E. F., Chu, A., and Holben, B. N., "Operational remote sensing of tropospheric aerosol over land from EOS moderate resolution imaging spectroradiometer," *Journal of Geophysical Research*, Vol. 102, pp. 17051-17067 (1997).
15. Kaufman, Y. J., Wald, A. E., Remer, L. A., Gao, B.-C., Li, R.-R., and Flynn, L., "The MODIS 2.1-μm channel – correlation with visible reflectance for use in remote sensing of aerosol," *IEEE Transactions on Geoscience and Remote Sensing*, Vol. 35, pp. 1286-1298 (1997).
16. Kiehl, J. T. and Briegleb, B. P., "The relative roles of sulfate aerosols and greenhouse gases in climate forcing," *Science*, Vol. 260, pp. 311-314 (1993).
17. Léon, J.-F., Chazette, P., Pelon, J., Dulac, F., and Randriamiarisoa, H., "Aerosol direct radiative impact over the INDOEX area based on passive and active remote sensing," *Journal of Geophysical Research*, Vol. 107, 8006, doi:10.1029/2000JD000116 (2002).
18. Liang, S., *Quantitative Remote Sensing of Land Surfaces*, John Wiley and Sons, New York, pp. 196-230 (2004).
19. Lin, C.-Y., Liu, S. C., Chou, C. C.-K., Liu, T. H., Lee, C.-T., Yuan, C.-S., Shiu, C.-J., and Young, C.-Y., "Long-range transport of Asian dust and air pollutants to Taiwan," *Terrestrial, Atmospheric and Oceanic Sciences*, Vol. 15, pp. 759-784 (2004).
20. Lin, C.-Y., Wang, Z., Chen, W.-N., Chang, S.-Y., Chou, C. C. K., Sugimoto, N., and Zhao, X., "Long-range transport of Asian dust and air pollutants to Taiwan: Observed evidence and model simulation," *Atmospheric Chemistry and Physics*, Vol. 7, pp. 423-434 (2007).
21. Lin, T.-H., Chen, A. J., Liu, G.-R., and Kuo, T.-H., "Monitoring the atmospheric aerosol optical depth with SPOT data in complex terrain," *International Journal of Remote Sensing*, Vol. 23, pp. 647-659 (2002).
22. Liu, C. H., Chen, A. J., and Liu, G. R., "An image-based retrieval algorithm of aerosol characteristics and surface reflectance for satellite images," *International Journal of Remote Sensing*, Vol. 17, pp. 3477-3500 (1996).
23. Liu, C. H. and Vermote, E. F., "A reflectance retrieval algorithm for landsat TM satellite image," *The 21st Asian Conference on Remote Sensing*, pp. 522-526 (2000).
24. Liu, G.-R., Lin, T.-H., and Kuo, T.-H., "Estimation of aerosol optical thickness by applying the optimal distance number to NOAA AVHRR data," *Remote Sensing of Environment*, Vol. 81, pp. 247-252 (2002).
25. Raut, J.-C. and Chazette, P., "Retrieval of aerosol complex refractive index from a synergy between lidar, sunphotometer and in situ measurements during LISAIR experiment," *Atmospheric Chemistry and Physics Discussions*, Vol. 7, pp. 1017-1065 (2007).
26. Remer, L., Kaufman, Y. J., Tanré, D., Mattoo, S., Chu, D. A., Martins, J., Li, R.-R., Ichoku, C., Levy, R. C., Kleidman, R. G., Eck, T. F., Vermote, E., and Holben, B. N., "The MODIS aerosol algorithm, products, and validation," *Journal of the Atmospheric Sciences*, Vol. 62, pp. 947-973 (2005).
27. Richter, R., "A spatially adaptive fast atmospheric correction algorithm," *International Journal of Remote Sensing*, Vol. 17, pp. 1201-1214 (1996).
28. Sifakis, N. I., Soulakellis, N. A., and Paronis, D. K., "Quatitative mapping of air pollution density using earth observations: A new processing method and application to an urban area," *International Journal of Remote Sensing*, Vol. 19, pp. 3289-3300 (1998).
29. Tanré, D., Deroo, C., Duhaut, P., Herman, M., Morcrette, J. J., Perbos, J., and Deschamps, P. Y., "Description of a computer code to simulate the satellite signal in the solar spectrum: 5s code" *International Journal of Remote Sensing*, Vol. 11, pp. 659-668 (1990).
30. Tanré, D., Deschamps, P. Y., Devaux, C., and Herman, M., "Estimation of saharan aerosol optical depth from blurring effects in thematic mapper data," *Journal of Geophysical Research*, Vol. 93, pp. 15955-15964 (1988).
31. Tanré, D., Herman, M., Deschamps, P. Y., and Leffe, A. de., "Atmospheric modeling for space measurements of ground reflectances, including bidirectional properties," *Applied Optics*, Vol. 18, pp. 3587-3594 (1979).
32. Wiscombe, W. J., "Improved Mie scattering algorithms," *Applied Optics*, Vol. 19, pp. 1505-1509 (1980).
33. Yang, C. M. and Chen., R. K., "Modeling rice growth using hyperspectral reflectance data," *Crop Science*, Vol. 44, pp. 1283-1290 (2004).